EVALUATION OF CONTAINMENT PEAK PRESSURE AND STRUCTURAL RESPONSE FOR A LARGE-BREAK LOSS-OF-COOLANT ACCIDENT IN A VVER-440/213 NPP

B. W. SPENCER, J. J. SIENICKI, R. F. KULAK, P. A. PFEIFFER[1], L. VÖRÖSS[2], Z. TÉCHY[3], AND T. KATONA[4]

1. Argonne National Laboratory, Argonne, IL 60439 USA
2. VEIKI Institute for Electric Power Research, Budapest, Hungary (current address: Hungarian Nuclear Regulatory Authority, Budapest, Hungary)
3. VEIKI Institute for Electric Power Research, Budapest, Hungary
4. Paks Nuclear Power Plant, Paks, Hungary

Abstract

A collaborative effort between U. S. and Hungarian specialists was undertaken to investigate the response of a VVER-440/213-type NPP to a "maximum design-basis accident", defined as a guillotine rupture with double-ended flow from the largest pipe (500 mm)in the reactor coolant system. Analyses were performed to evaluate the magnitude of the peak containment pressure and temperature for this event; additional analyses were performed to evaluate the ultimate strength capability of the containment. Separate cases were evaluated assuming 100% effectiveness of the bubbler-condenser pressure suppression system as well as zero effectiveness. The pipe break energy release conditions were evaluated from three sources: 1) FSAR release rate based on Soviet safety calculations, 2) RETRAN-03 analysis and 3) ATHLET analysis. The findings indicated that for 100% bubbler-condenser effectiveness the peak containment pressures were less than the containment design pressure of 0.25 MPa. For the BDBA case of zero effectiveness of the bubbler-condenser system, the peak pressures were less than the calculated containment failure pressure of 0.40 MPa absolute .

I. INTRODUCTION

One of the basic issues of reactor safety is the ability of the reactor containment to withstand the loadings of design basis accidents (DBAs) and even beyond design basis accidents (BDBAs). Typically, the design of the containment has been specified to withstand the containment peak pressure and temperature conditions for a spectrum of design basis accidents including the guillotine rupture of the largest pipe in the reactor coolant system. This latter accident, commonly called a large-break loss-of-coolant accident (LBLOCA) or the "maximum DBA", typically results in maximum pressure loading of the containment and is often the defining event for specification of the containment design pressure. Following the accident at TMI-2, there was a major effort in the U.S. to quantify the magnitude of containment loads as well as the strength capability of the various containment designs to evaluate what, if any, margins to failure exist [1, 2].

The objective of the present work was to address containment failure margin for a generic

DISCLAIMER

VVER-440/213 for the maximum DBA by evaluating the corresponding pressure and temperature loadings in the containment and additionally evaluating the strength capability of the containment structure and its boundary.

The VVER-440/213 containment design features a bubbler-condenser tower with water trays for the suppression of steam pressure resulting from a pipe break accident (Fig. 1). The bubbler-condenser tower contains twelve levels of water trays. The nominal water depth in the trays is 0.5 m and the total water volume is 1500m^3. In the event of a pipe break accident, the steam-air mixture flows horizontally from the steam generator compartment through a steam corridor to the vertical tower. The steam-air mixture enters the twelve levels of water trays through arrays of slots on the underside which channel the mixture into the bottom of the water pools. The steam is condensed in these water pools. Noncondensable gas (primarily air and hydrogen) is displaced from the tray enclosures into the adjacent air traps by means of one-way "flapper-type" valves. Steam in the containment atmosphere is further condensed by operation of the containment sprays at a later time. The effectiveness of the bubbler-condenser system to reduce peak containment pressure has not been tested at large scale. Hence the issue of bubbler-condenser effectiveness was one of the areas of focus in this study.

This work was carried out at ANL using the existing PACER containment loads code [3] and the NEPTUNE structural strength code [4], both of which were previously used for the 1987 U.S. DOE study of safety aspects of VVERs [5]. Both codes relied on system, configuration, and materials information available in the West at that time. The codes were modified where needed for this study using realistic input information to create generic VVER-440/213 models. This work was documented in its entirety in a 1996 U.S. DOE report [6].

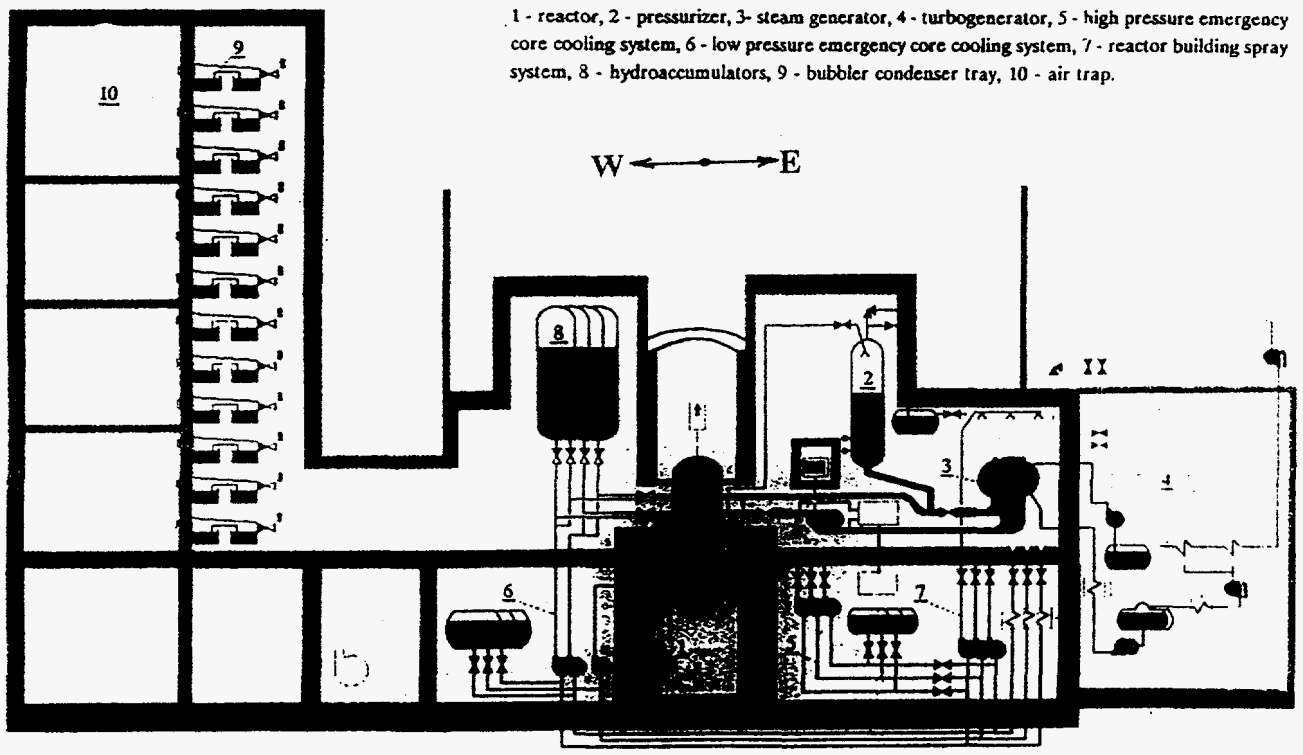

Fig. 1 Illustration of VVER-440/213 Containment

The PACER analyses included use of break flow conditions from three sources: a) a Final Safety Analysis Report (FSAR) based on Soviet safety analysis, b) RETRAN-03 calculations performed in 1987 at Brookhaven National Laboratory [5], and c) German ATHLET code calculations performed by the Hungarian Atomic Energy Research Institute (KFKI). These LBLOCA analyses show considerable difference in predicted break flow conditions, and hence the PACER results illustrate the sensitivity of the calculated peak containment pressure to the range of break flowrates. There was no attempt to mechanistically calculate the condensation of steam in the steam-air mixture passing through the water pools. The uncertainty in the condensation was handled in PACER by assumptions intended to bracket the actual behavior. That is, two cases of bubbler-condenser effectiveness were considered, 0% and 100%, where effectiveness is defined here as the percentage of steam passing through the water pools that is actually condensed. Hence, the PACER results illustrate the difference in containment pressure calculated assuming perfect, as-designed functioning of the condensers, as well as a BDBA case of no condensation effect whatsoever.

The NEPTUNE analyses included evaluation of the reinforced concrete structures of the containment including the steam generator compartment, motor compartment, reactor shaft, bubbler-condenser tower, and air trap regions. In addition, penetration covers were examined including: a) the hermetic cap atop the reactor shaft, b) the sluice gate between the reactor shaft and the refueling pool, c) equipment hatch covers in the containment ceiling, and d) various doors. The structural analysis did not include consideration of any potential failures inside the containment, such as buckling of the bubbler-condenser trays themselves under differential pressure associated with the LBLOCA loads, since that would not affect the containment boundary per se, and since its effect on internal pressure was bracketed by the BDBA assumption of 0% bubbler-condenser effectiveness in analysis cases.

II. CONTAINMENT LOADS ANALYSIS

Because the PACER code was specifically developed for applications to VVERs, models for key features of the VVER-440/213 plants such as the bubbler-condenser structures, corridor, and the check valves were incorporated into the formulation of the code from the outset [5]. The containment is represented as a user-defined set of interconnected cells. Each cell represents either a single compartment, or an aggregation of several compartments. For each such cell, a cell volume and surface area are specified for the condensation of steam. The interconnections between the various cells were defined together with flow areas, flow contraction coefficients, and logic describing the functioning of valves (such as the check valves leading to the air traps) and rupture discs. Sources for steam and water addition to a cell such as those associated with coolant discharge from the ruptured primary pipe are defined. Specific pressure mitigation systems such as bubbler-condenser trays or water droplet sprays can be defined within any cell.

During the primary system blowdown, the steam-air mixture contains entrained water droplets in thermal equilibrium with the gas-vapor phase. The flowrate from one compartment to another is calculated assuming isentropic flow and an expression for the relative mass fractions of water droplets and gas-vapor mixture flowing between the compartments. The droplet carryover fraction is given by an expression of Schwan based upon analysis of experiment data from the Battelle Frankfurt and Marviken containment loading experiments [7]. In the cell in which the pipe break is located, all of the water from coolant discharge is assumed to enter the cell atmosphere as entrained droplets.

Water droplets carried with steam and air into the bubbler-condenser suppression pool trays are assumed to be retained in the water pools. The modeling of bubbler-condenser behavior includes calculation of the downward expulsion of water from the downward facing trays that must occur before steam and air can begin to rise through the upward facing trays. When the bubbler-condenser

tray water is subcooled, all of the steam entering the trays has been assumed to be condensed. If the tray water is heated to the saturation temperature, then that fraction of the steam entering the pool is condensed that maintains the tray water in a saturated state. In order to investigate less than ideal functioning of the bubbler-condenser trays, some cases considered that only a fraction (for example, zero) of the steam entering subcooled water in the trays is condensed.

PACER calculates the condensation of steam upon structure and equipment using the correlations of Schauer that are based upon analyses of the HDR, Marviken, and Battelle Frankfurt containment loading experiments [8]. Two distinct correlations describe condensation during, respectively: i) the blowdown phase and the period shortly thereafter when forced convection effects are important; and ii) the post-blowdown period when natural convection dominates the condensation transport processes. For the present analysis, the effects of the thermal resistance of structure upon the condensation rate are approximated in terms of expressions for the effective thermal resistance of the steel liner plates and the concrete behind the liner.

Containment Nodalization

Figure 2 shows the nodalization of the VVER-440/213 containment used in the PACER calculations. The containment was represented by twenty cells. Two cells were used to represent the steam generator compartment. This reflects the greater area for flow into the respective portions of the horizontal corridor leading to the bubbler-condenser tower than the area for flow between the two halves of the steam generator compartment. In order to distinguish between the two steam generator compartment halves, an orientation was defined such that the containment is on an east-west line with the bubbler-condenser tower to the west and the steam generator compartment to the east. The two cells representing the steam generator compartment are therefore the north and south halves. The break is assumed to occur inside the steam generator compartment south portion and in the primary coolant loop that is located nearest to the cable room on the east wall. This is a conservative assumption in that the flow area from the south half of the steam generator compartment into the south portion of the corridor is less than the corresponding area from the north half into the north portion of the corridor. This wili result in slightly higher pressures for a break located in the south side.

The north and south portions of the horizontal corridor to the bubbler-condenser tower are separated by a vertical wall and are therefore represented by separate cells. The flow areas connecting each portion of the horizontal corridor to the ventilation center correspond to that of the intake ducts rising above the corridor floor. The pump motor compartment, reactor shaft, ventilation center, and various other compartments are aggregated into a single cell in the nodalization. During the blowdown phase, air and steam flow into these compartments and tend to be "dead ended" in them. The aggregated cell volume is connected with both the north and south portions of the steam generator compartment and the horizontal corridor. The nodalization of the bubbler-condenser tower defines an individual cell for each of the four air traps. A single cell is also defined to represent the three levels of bubbler-condenser trays (containing 375 m^3 water on average) and tray enclosures associated with each air trap. The nodalization accounts for the minor differences in volumes and areas between different levels inside the tower.

Calculation of Containment Loadings

An assessment of maximum DBA loadings for the VVER-440/213 was carried out using the break flow conditions obtained from system thermal hydraulics codes ATHLET and RETRAN-03. The break flowrate conditions used in a V213 FSAR, based on Soviet safety analyses, were also used. The break flowrates are shown in Fig. 3. The peak flowrates are 25500, 17500, and 14000 Kg/s for the FSAR, ATHLET, and RETRAN cases, respectively, based on a cold leg break. The peak flowrate calculated by RETRAN for a hot leg break was 8500 Kg/s.

Fig. 2 PACER Nodalization for VVER-440/213; Break is located in Cell 1.

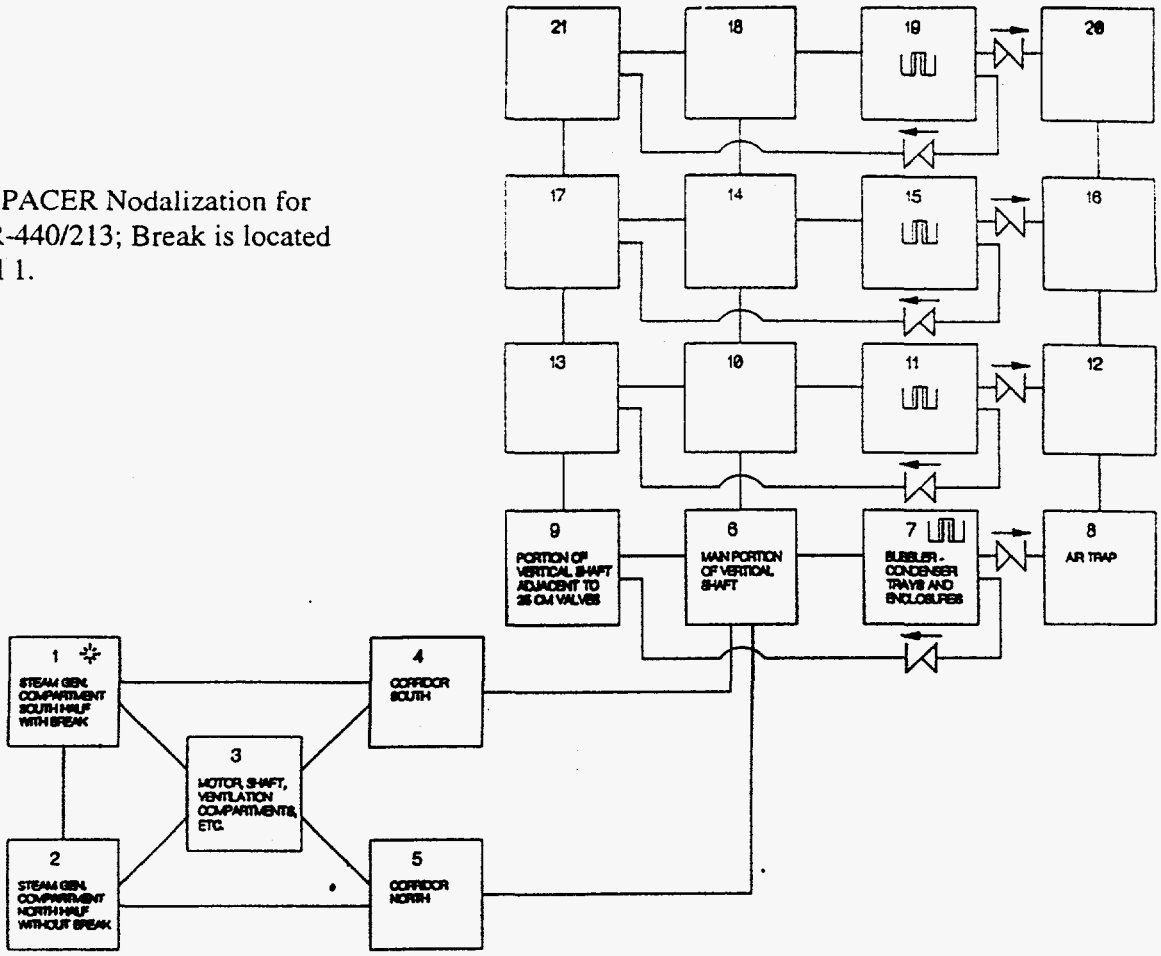

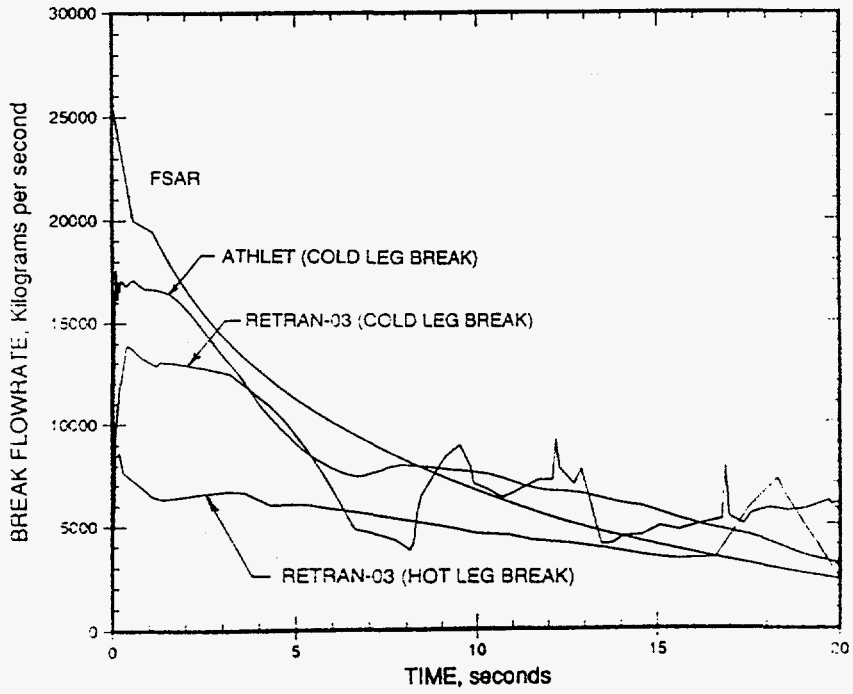

Fig. 3 Break Flowrate Conditions Used in PACER Analyses.

Pressure and temperature loadings calculated for the ATHLET break conditions are shown in Figs. 4a and 4b, respectively. The pressures and temperatures are presented inside four cells together with the cell number designation. The first (Cell No. 1) is the south portion of the steam generator compartment in which the break is located. Cell 16 represents the third air trap above the bottom of the bubbler-condenser tower. Cell 15 models the bubbler-condenser trays and tray enclosures of the three levels of trays that are associated with this air trap. Cell 14 corresponds to the major portion of the vertical shaft inside the bubbler-condenser tower that encompasses the three tray levels. The maximum pressure loading of 0.203 MPa (all pressures are absolute) is calculated to occur inside the steam generator compartment at 4 seconds following inception of the break. The peak temperature of 120 C is also calculated inside the steam generator compartment at this time. This temperature is equal to the local saturation temperature at the partial pressure exerted by the steam. The peak pressure calculated inside the vertical shaft of the bubbler-condenser tower at Cell 14 is observed to be 0.187 MPa.

The nodalization of the bubbler-condenser tower represents each of the four individual air traps with distinct cells. For each air trap, a single cell represents the three levels of bubbler-condenser trays and tray enclosures that discharge into the air trap. Because the air traps and aggregates of tray enclosures do not have identical volumes and because the tray levels are located sequentially along the height of the tower vertical shaft, the pressures attained inside the various tray enclosures and air traps are not equal. The calculated time dependent pressures are shown in Figs. 5a and 5b. The middle two air traps corresponding to Cells 12 and 16 have less volume than the other two air traps. The pressures inside the middle two air traps are thus calculated to be greater than the pressures in the bottom and top air traps. Because the middle two air traps have equal volumes, virtually indistinguishable pressures are calculated for these two air traps. The pressures inside the bottom and top air traps which do not have identical volumes are very close to one another. Virtually no difference in pressure is calculated between the cells comprising the vertical shaft within the bubbler-condenser tower. Thus, the walls of the vertical shaft are subjected to essentially a uniform loading along the height of the shaft. Differences in pressure between the four air traps and between the various tray enclosures approach zero after 20 seconds when most of the primary coolant system blowdown has occurred. In the VVER-440/213 design, successive air traps are connected by an open hole in the air trap floor that allows water to drain to the floor of the lowest trap. The calculations show that these drain openings are large enough to equilibrate the pressures in all of the air traps within 20 seconds.

The calculated peak pressures and temperatures in the steam generator compartment and in the bubbler-condenser tower are summarized for the four cases of blowdown flowrate conditions in Table 1. As can be seen, the calculated peak pressures decrease for cases of decreasing maximum break flowrate, attributable to the effect of various sources of condensation in the containment. The peak pressure loading inside the bubbler-condenser tower vertical shaft is typically less than that inside the steam generator compartment. Results of these analyses indicate peak pressures below the 0.25 MPa containment design pressure for all cases of LBLOCA break flowrate conditions.

To determine the sensitivity of the calculated peak pressures to the effectiveness of steam condensation in the bubbler-condenser trays, cases were run in which it was assumed that water remained inside the trays, but steam passes through the water without any condensation. This is the limiting case of condenser ineffectiveness (0% efficiency). Results of these calculations are also shown in Fig. 4a and Table 1. For the reference ATHLET break flowrate, the peak pressures in the steam generator compartment and bubbler-condenser shaft were 0.305 MPa. While this value exceeds the containment design pressure of 0.25 MPa, it does not mean that containment boundary failure will occur. The pressure at which such failure might occur is addressed in the next section.

The PACER calculations of peak containment pressure were compared with analogous calculations performed by VEIKI using the CONTAIN 1.1 code. The specific case used the FSAR

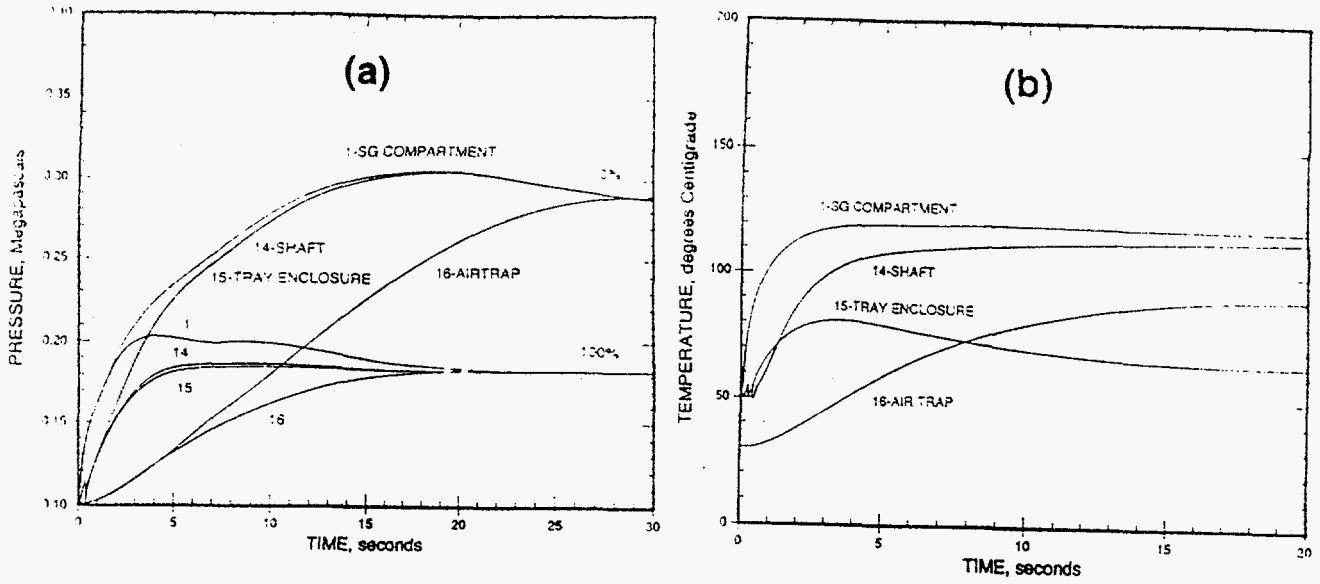

Fig. 4 Pressure Loadings (a) and Temperature Loadings (b) Calculated with PACER for ATHLET Cold Leg Break Conditions; 0% and 100% Effectiveness of Bubbler-Condensers.

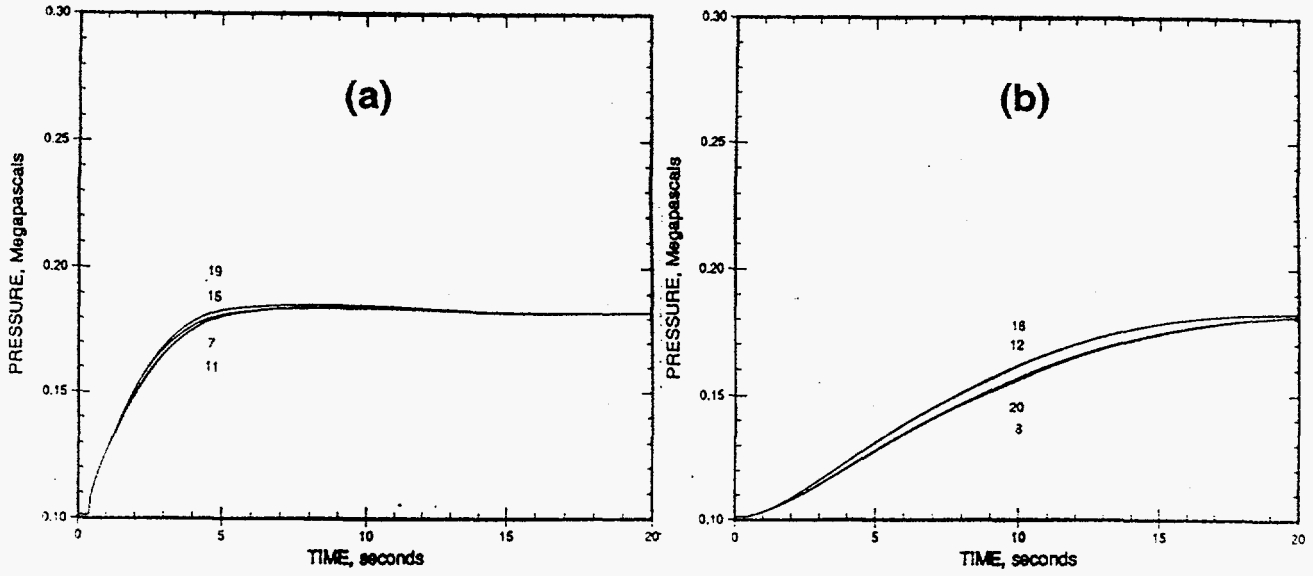

Fig. 5 Pressure Loadings Inside Bubbler-Condenser Tray Enclosures (a) and Inside Air Traps (b) for ATHLET Cold Leg Break Conditions: 100% Effectiveness of Bubbler-Condensers.

Table 1. Comparison of Calculated Peak Containment Pressure and Temperatures

Source of Blowdown Flowrate	Steam Generator Compartment Peak Pressure, MPa (Temp. C)		Bubbler/Condenser Tower Peak Pressure, MPa (Temp. C)	
Bubbler-Condenser Efficiency	100%	0%	100%	0%
FSAR	0.235 (125)	0.362 (140)	0.205 (117)	0.362 (135)
ATHLET (Cold Leg Break)	0.203 (120)	0.305 (133)	0.187 (113)	0.305 (129)
RETRAN-03 (Cold Leg Break)	0.197 (119)	0.248 (127)	0.181 (110)	0.247 (120)
RETRAN-03 (Hot Leg Break)	0.178 (117)	0.248 (127)	0.175 (113)	0.248 (120)

blowdown flowrate and assumed 100% effectiveness of the bubbler-condenser. The peak pressure was calculated to be 0.235 MPa using PACER versus 0.213 MPa using CONTAIN. To address the reason for this difference, a version of PACER was written incorporating steam formation assumptions similar to CONTAIN. Specifically, the CONTAIN 1.1 approach effectively equilibrates the released coolant with the entire steam-water mass inside the cell atmosphere prior to the determination of steam formation. This approach tends to reduce the steam mass that is calculated to be formed. With the revised version of PACER, the peak containment pressure was reduced from 0.235 MPa to 0.218 MPa, in reasonably good agreement with the CONTAIN 1.1 value of 0.213 MPa. It should be noted that the PACER approach to modeling steam formation and expansion work was judged to be a more realistic representation of the heat and mass transfer thermodynamic processes taking place inside a large volume steam generator compartment. PACER flashes released coolant and subsequently equilibrates it with the existing steam/air mixture inside the compartment atmosphere. The traditional approach that thermally mixes the unexpanded coolant upstream of the break with the compartment atmosphere might be expected to hold in the limit of a small nodal volume immediately surrounding the break location and much smaller in size than the nodes used to represent the V213 containment.

III. CONTAINMENT STRUCTURAL STRENGTH

The objective of this work was to evaluate the ultimate pressure capability of the confinement structures and to identify probable failure locations. The NEPTUNE three-dimensional, nonlinear finite element code was used to calculate the response of the reinforced-concrete structural compartments of the containment to overpressure. The containment system consists of two interconnected main structures: the accident localization compartments and the bubbler-condenser tower, connected by a corridor. The accident localization compartments contain the reactor, pumps, motors, steam generators, pressurizer, accumulators, and associated piping. The bubbler-condenser tower contains a vertical shaft, racks of bubbler-condenser trays, and four air trap compartments.

The reactor is positioned in the reinforced concrete cylindrical reactor shaft made of heavy concrete. The bottom of the shaft is sealed by the 2.3 m thick basemat. The top of the shaft is sealed by a steel cap, which is part of the hermetic boundary. The annular-shaped motor room surrounds the upper reactor shaft up to the operating floor. The motor room is supported by 14 reinforced concrete columns at its outer periphery. The columns are anchored to the steam generator compartment floor. The latter is a box-like reinforced concrete structure with the following outside dimensions: 48 m long, 39 m wide, and 11 m high. Its 1.5 m (4.9 ft) thick floor is made of reinforced concrete. The operating floor, which is the ceiling of the steam generator compartment, is also 1.5 m thick reinforced concrete. The west wall has two openings that lead into the corridor between the steam generator room and the bubbler-condenser tower. The main walls of the steam generator compartment are 1.5 m thick reinforced concrete, except for the side wall that is adjacent to the adjoining unit. This side wall is constructed of 1.0 m thick reinforced concrete.

The other main confinement structure is the 40 m wide, 32 m deep, and 40 m high bubbler-condenser tower. The outside walls and roof are made from reinforced concrete that is 1.5 m thick. A 1.5 m thick interior wall divides the structure into two parts. The eastern part contains 12 levels of bubbler-condenser trays that are supported on 216 steel I-beams. Each I-beam has a web that is 560 mm high and 12 mm thick and a flange that is 200 mm wide and 20 mm thick. The I-beams are securely anchored to the east exterior wall and the interior wall. (Note, in early designs the beams may not have been securely anchored to the walls in which case the beams did not provide any support between the east exterior wall and the middle wall.) The east wall has openings to the corridor from the steam generator compartment. The western part is divided into four airtraps by 1.0 m thick reinforced concrete floors.

The walls, floor slabs, and ceiling slabs, with some exceptions noted below, have a stainless steel liner affixed to both their inside and outside surfaces. The surfaces that are designated to be the hermetic boundary have a special collection system at the seam welds to monitor leaks. The largest part of the hermetic boundary consists of 6 mm thick stainless steel sheets affixed to or embedded in the concrete walls, floor slabs, and roof slabs. The other parts of the hermetic boundary are doors, hatch covers, reactor shaft cap, and sluice gates.

Methodology for Structural Analysis

The analysis of large, complex reinforced-concrete structures requires the use of accurate and numerically efficient finite elements. An element that has most of the desired features was developed by Belytschko, et. al.[9]. The element was further developed by Kulak and Fiala [4] by incorporating features to represent concrete and reinforcing steel. Subsequently, additional failure criteria were added, and now the NEPTUNE element can model concrete cracking, rebar failure, and gross transverse failure. The concrete failure model utilized is the Hsieh-Ting-Chen (H-T-C) four-parameter model [10]. The strength capacity of the concrete in a multiaxial stress space can be characterized by the H-T-C four-parameter failure surface. The concrete response after failure is simulated using the element size independent cracking criterion established by Bazant and Oh [11].

Additionally, the transverse shear failure of a reinforced concrete slab is also considered by use of an empirical formula. These types of failure occur at junctures and corners, such as the wall and floor interfaces, wall and basemat junctures, etc. Aoyagi and Yamada [12] have estimated the ultimate strength in shear for the reinforced concrete sections based on experimental data.

Material Properties for Structural Analysis

Best estimate material properties were obtained from handbooks and used in the analyses. Two types of concrete were used in the construction of the VVER-440/213. Normal weight concrete with a compressive strength and yield strength of 27 MPa and 13.5 MPa, respectively, was used for the most of the walls and floor slabs. The tensile strength was taken to be 1.89 MPa and the ultimate strain was 0.003 mm/mm. Heavy weight concrete was used for radiation shielding in the reactor shaft and for the east wall of the steam generator compartment. It had a compressive strength and yield strength of 34.5 MPa and 17.3 MPa, respectively, a tensile strength of 2.42 MPa, and an ultimate strain of 0.003 mm/mm. Young's Modulus was 25.0 and 28.0 GPa for the normal and heavy concrete, respectively; Poisson's Ratio was 0.18.

The diameters of the reinforcing steel used in the localization compartments were 16 mm, 25 mm, 28 mm, 32 mm, and 40 mm. The rebars were all deformed bars with a carbon content of 0.22%. The yield stress was 333 MPa and the ultimate stress was 588 MPa. The ultimate strain was taken to be 20%. The Young's Modulus was 200 GPa. The failure strain in tension was assumed to be at 5% strain, due to the connections of rebar ends. The rebar spacing ranged from 100 mm to 300 mm. The main structural rebars in the hermetic boundary were 40 mm, and their spacing ranged from 150 mm to 300 mm.

The steel used for the 6 mm thick liner was type A38B having material properties: the elastic modulus was 199 GPa; the yield stress was 235 MPa; and the ultimate strength was 370 MPa. The uniaxial ultimate strain was taken to be 20%.

Calculation of Structure Strengths

Finite element structural response simulation were performed for the accident localization compartments and the bubbler-condenser tower. Decoupled three-dimensional models for these two structures were developed and independently subjected to internal pressure loading. Temperature loadings were not taken into account.

A three-dimensional finite-element model (Fig. 6a) was constructed for the accident

localization compartments and their underlying supporting structures. The model includes the motor room, steam generator compartment, reactor shaft; storage pond, transfer pond, superstructure above the reactor shaft and ponds, pressurizer and accumulator structures, operating floor, and supporting substructures. The model consists of 3545 finite elements (3519 quadrilateral elements and 26 beam elements) and 3302 nodes with a total of 19,812 degrees of freedom. The supporting columns are modeled with three-dimensional beam elements. The thickness of the non-pressurized supporting sub-walls varied from 0.8 m to 1.5 m.

Detailed structural response calculations were carried out to the point of gross structural failure using the NEPTUNE code. The interior surfaces of the hermetic boundary were incrementally pressurized in 0.04 MPa load steps until structural failure was indicated. The displacement histories indicate that the compartments responded linearly up to a pressure of 0.30 MPa. Nonlinear response is evident beyond a pressure of 0.30 MPa as cracking initiates and propagates over larger and larger regions of the walls and through the thickness. The first structural failure was predicted to occur at a pressure of 0.46 MPa. The failure was a shear failure in the steam generator floor at inner wall and support column locations. Additional shear failures occurred progressively in the pressure range 0.50-0.66 MPa. These failures were based on the criterion developed by Aoyagi and Yamada. This criterion takes into account the strength of the reinforcement steel. (Note, a failure criterion that did not allow the strength of transverse rebars to be considered would have predicted a first shear failure at a pressure of 0.30 Mpa.) The first failure on a side wall of the accident localization compartment was also a shear failure and was predicted at 0.70 MPa.

A three-dimensional finite-element model (Fig. 6b) was also constructed for the bubbler-condenser compartments and their underlying supporting structures. The model includes the vertical

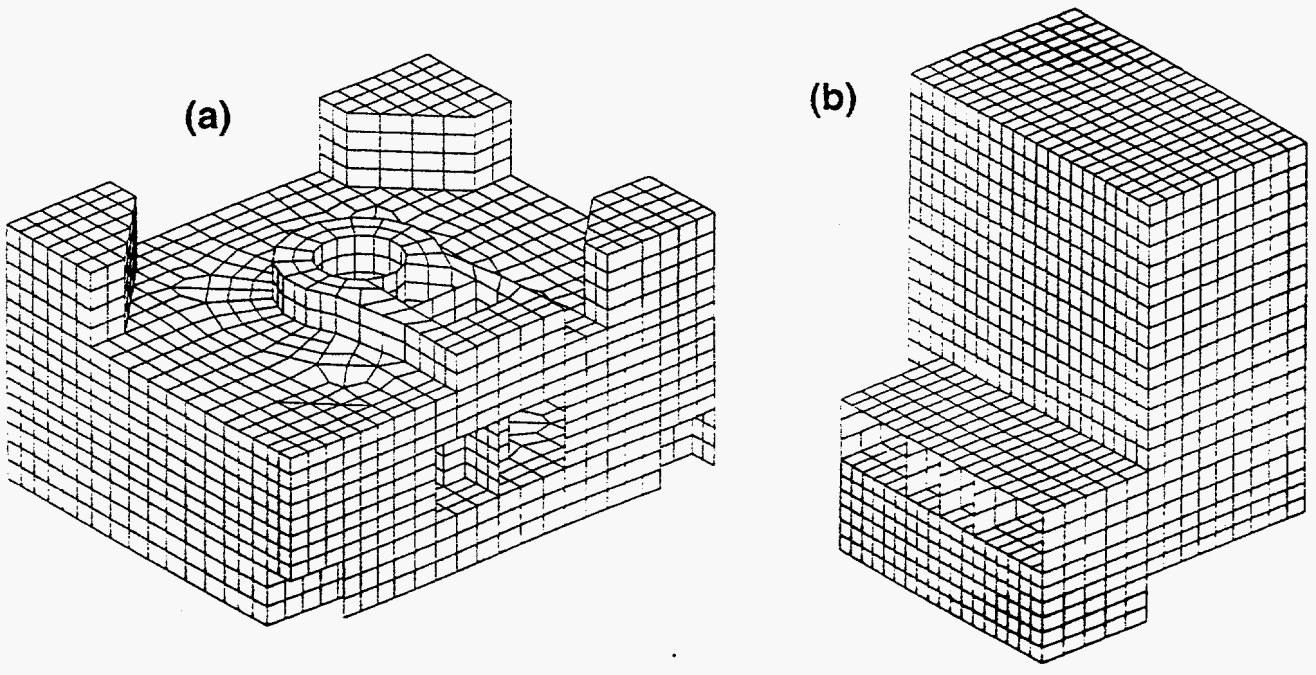

Fig. 6. NEPTUNE Finite Element Models of the Accident Localization Compartments (a) and the Bubbler-Condenser Tower (b).

tower (with trays), four airtraps, the corridors that connect to the accident localization compartments, supporting substructures, and the supporting beams of the condenser trays. The beams spanning between the interior wall and the east exterior wall of the bubbler tower were assumed rigidly anchored at the walls, thereby tying the walls together. The total number of nodes was 2696 with 2829 quadrilateral elements for reinforced concrete and 228 beam elements for the support of the condenser trays. The supporting beams were modeled with three-dimensional beam elements. The thickness of the non-pressurized supporting sub-walls varied from 0.6 m to 1.5 m. The interior surfaces of the hermetic boundary were incrementally pressurized in 0.02 MPa load steps. The displacement histories indicate that the compartments responded linearly up to a pressure of 0.24 MPa. Nonlinear response was evident beyond a pressure of 0.24 MPa as cracking initiates and propagates over larger and larger regions of the walls and through the thickness. The first structural failure was predicted to occur at a pressure of 0.40 MPa. The failure was a shear failure in the roof of the top airtrap at the sidewall/roof junctures near the middle wall. The corresponding outward displacement of the center of the roof was calculated to be 0.18 m. The failure criterion took into account the strength of the transverse reinforcement steel. (Note, a failure criterion that did not allow the strength of transverse rebars to be considered would have predicted this shear failure at a pressure of 0.26 MPa.) The calculations were allowed to continue past this initial failure point. Additional shear failures were predicted at 0.42 MPa at the sidewall/roof juncture near the middle on the bubbler-condenser (tray) side of the tower. The first rebar failure in tension was predicted at a pressure of 0.44 MPa. This failure occurred in the roof of the top airlock at a central location midway between the walls.

An additional analysis was done for the bubbler-condenser tower building for the case that the condenser tray support beams are not rigidly anchored at the middle and east exterior walls of the tower; i.e., the beams are simply supported at the wall brackets. The first structural failure was predicted to occur at a pressure of 0.22 MPa. The failure was a rebar failure in tension of the large unsupported east exterior wall of the bubbler-condenser tower.

Analyses were additionally performed for other boundary elements including the shaft hermetic cap, hatch covers in the floor of the operating deck, sluice gates in the fuel transfer path, and doorways. The results indicated that none of these elements is likely to fail structurally at less than the 0.40 MPa pressure evaluated for the reinforced-concrete structures. Details are presented in Ref. 6.

IV. SUMMARY OF FINDINGS

An independent assessment of the peak containment loads for the maximum DBA was carried out with PACER assuming break conditions calculated with the FSAR, ATHLET, and RETRAN-03 thermal hydraulics codes. The peak pressure loadings calculated for 100% effectiveness of the bubbler-condenser system ranged from 0.178 MPa to 0.235 MPa in the steam generator compartment and 0.175 MPa to 0.205 MPa in the bubbler-condenser tower. These pressures are all less than the containment design pressure of 0.25 Mpa absolute

The peak pressure loadings for the postulated BDBA case which assumes 0% effectiveness of the bubbler-condenser system ranged from 0.248 MPa to 0.362 MPa in the steam generator compartment as well as in the bubbler-condenser tower. These pressures are less than the maximum containment pressure capability calculated by NEPTPUNE to be 0.40 Mpa absolute. The containment failure location was calculated to occur in the roof-wall junction of the top airlock. Since the largest pressure for the pipe break accident is developed in the steam generator compartment, it is worth noting that the pressure capability in that compartment was calculated to be 0.46 MPa, notably larger than the pressure capability calculated in the tower/airtrap region. These findings are based on a VVER-440/213 having I-beams in the bubbler-condenser tower (which

support the water trays) anchored rather than freestanding at their wall supports.

ACKNOWLEDGMENT

This work was sponsored by the U.S. Department of Energy under Contract No. W-31-109-Eng-38.

REFERENCES

1. "Containment Performance Working Group Report," U.S. NRC, NUREG-1037 (1985).
2. "Estimates of Early Containment Loads, U.S. NRC, NUREG-1079 (1985).
3. J. J. Sienicki, "PACER-A Fast Runnin"g Computer Code for Calculation of Short-term Containment Loads Following Coolant Boundary Failure, V.1: Code Models and Correlations," ANL-NT-40 (1997).
4. R. F. Kulak and C. Fiala, "NEPTUNE: A System of Finite Element Programs for Three-Dimensional Nonlinear Analysis," *Nuclear Engineering and Design,* Vol. 106, No. 1, pp. 47-68 (1988).
5. "Department of Energy's Team Analyses of Soviet Designed VVERs," DOE/NE-0086, Rev. 1, Main Report, Analysis Appendix C, United States Department of Energy (1989).
6. "Containment Loads and Structural Response for a Large Pipe Break Accident in a VVER-440/213 Nuclear Power Plant," U.S. DOE, Office of Nuclear Energy, Science, and Technology, (September 1996).
7. H. B. Schwan, "Containment Code Verification by Systematic Evaluation of Experimental Data," *Thermal-Hydraulics of Nuclear Reactors, Proceedings of the Second International Topical Meeting on Nuclear Reactor Thermal-Hydraulics*, Santa Barbara, California, January 11-14, 1983, Vol. II, p. 1052, American Nuclear Society, La Grange Park (1983).
8. D. A. Schauer, "Transient Condensation Heat Transfer Coefficient Expressions During and After Blowdown," *Fifth International Meeting on Thermal Nuclear Reactor Safety*, Karlsruhe, Federal Republic of German, September 9-13, 1984, KFK 3880/3, Vol. 3, p. 1850, Kernforschungszentrum Karlsruhe (December 1984).
9. T. Belytschko, J. I. Lin, and C. Tsay, "Explicit Algorithms for the Nonlinear Dynamics of Shells," *Computer Methods in Applied Mechanics and Engineering,* Vol. 42, pp. 225-251 (1984).
10. S. S. Hsieh, E. C. Ting, and W. F. Chen, "An Elastic-Fracture Model for Concrete," *Proceedings, 3rd Engineering Mechanics Division Specialists Conference, ASCE,* Austin, TX, pp. 437-440 (1979).
11. E. P. Bazant, and B. H. Oh, "Crack Band Theory for Fracture of Concrete," *Material Struct.,* RELEM, Paris, France, Vol. 16, pp. 155-177 (1983).
12. Y. Aoyagi and K. Yamada, "An Experimental Approach to the Design of Network Reinforcement Against In-Plane Shear in Reinforced Concrete Containments," *Proceedings of Structural Mechanics in Reactor Technology,* Vol. J 4/7, pp. 1-10 (1979).